The Journal of Experimental Biology **198**, 1469–1481 (1995)
Printed in Great Britain © The Company of Biologists Limited 1995

THE DISTAL SPERM FLAGELLUM: ITS POTENTIAL FOR MOTILITY AFTER SEPARATION FROM THE BASAL STRUCTURES

D. M. WOOLLEY AND H. H. BOZKURT

Department of Physiology, School of Medical Sciences, University of Bristol, University Walk, Bristol BS8 1TD, UK

Accepted 6 March 1995

Summary

The distal region of the sperm flagellum of *Gallus domesticus* has been separated and purified. It consists of a 9+2 axoneme, without basal or accessory structures. Such distal segments have been demembranated and then reactivated, either by adding ATP or by releasing ATP photolytically from caged ATP: we find that they are capable of a period of independent motility. Bends form repetitively and travel towards the tip, though it is an abnormal, irregular pattern of beating. It is argued that this motility is not dependent on damage to the flagellum at the fracture site. Evidence is presented that the potential for such motility depends upon the existence of bends on the axoneme before the reactivation. The reactivated motility is short-lived: 50 % of the distal flagellar segments, placed in the reactivating solution, become quiescent and straight within 60 s. However, vigorous beating can be induced in such quiescent segments of axoneme by compressing one end with a glass microneedle. We record, provisionally, that the site of compression does not determine the direction in which bends move along the flagellar segment. The effect of compression in re-initiating motility suggests that a mechanical resistance is necessary, somewhere along the axoneme, for normal, sustained motility; it is proposed that the specialized basal structures, collectively, provide such a resistance in the intact flagellum.

Key words: flagella, cilia, basal body, centriole, sperm tail, sperm motility, caged ATP, dynein, *Gallus domesticus.*

Introduction

The basal region of the eukaryotic flagellum and the cilium always contains specialised structures. In most cases there is a basal body (or distal centriole), which may or may not have anchorages associated with it, and distal to this, there are the various structures within the transition zone. The basal body itself, in terms of its centriolar architecture, cannot be essential for axonemal beating. The evidence for this statement includes the results of numerous flagellar microdissection experiments and ciliary and flagellar abscission experiments in which beating has been verified in portions of axonemes free of basal bodies (Terni, 1933; Goldstein *et al.* 1970; Lindemann and Rikmenspoel, 1972; Douglas and Holwill, 1972; Goldstein, 1974; Okuno and Hiramoto, 1976; Hoops and Witman, 1985). Furthermore, the basal bodies of some flagella degenerate after the development of the axoneme, yet such flagella are motile (Fawcett and Phillips, 1969; Baccetti, 1972).

However, there have been some reports that when sea urchin spermatozoa are broken by laser microbeam, by fluid shear or with a homogenizer, the separated distal segments lose the ability to bend or beat in the presence of ATP (Goldstein, 1969; Gibbons and Gibbons, 1972; Kamimura and Kamiya, 1989). In the work of Brokaw and Benedict (1968), the loss of motility was described as almost complete. This suggests that in the spermatozoa studied some component or attribute of the basal region is necessary for the motor function of the distal flagellum: in its absence, the flagellar segments were said to be ‘quiescent’ (Kamimura and Kamiya, 1989).

One way to reconcile these two sets of observations is to make the hypothesis that the basal region contributes a functionally important mechanical resistance, rather than any specific structure. For this idea to conform with earlier experimental results, certain re-interpretations of them become necessary; namely (1) that in the reported microdissection and similar experiments, the mode of cutting the flagellum had set up new and effective structural linkages between the axonemal structures at the injury site; and (2) that in the relevant ciliary abscission experiments, the position of the breakage point had meant that transition zone linkages remained with the detached axoneme and permitted continued motility. The plausibility of these additional suggestions will be discussed.

The idea that a system of basal linkages is functionally important is not new. Machin (1963) considered that proximal impedances would establish propagation direction; Douglas and Holwill (1972) obtained experimental evidence favouring this view. Also, a restriction on basal displacements has been a condition both of computer simulations of flagellar motility (since the work of Brokaw, 1972) and of the many calculations of sliding displacements based on sliding filament theory (e.g. Gibbons, 1981).

In this work, we examine the hypothesis that there is a

functional requirement for a system of basal linkages. We have chosen to study a sperm flagellum, from which it is possible to detach, by vortex-shear, a distal segment of 9+2 axoneme, free of basal or accessory structures. We have tested the potential for motility of these distal segments in the presence of ATP. By releasing the ATP photolytically from caged ATP, we have been able to observe reactivation from its initiation. In fact, the segments do show spontaneous, independent motility, but only transitorily; then they become quiescent. (This complex response may explain some of the disagreement in the literature.) Having obtained detached flagellar segments in the quiescent state, we have proceeded to question whether this quiescence is due to the lack of resistive structures at one end of the segment. This has been tested by compressing one end with a glass microneedle, thus crudely preventing or impeding intra-axonemal movements. It has been found that this intervention does indeed permit a further period of beating. These experiments will be presented in detail and discussed. Finally, we advance the theory that, in the normal flagellum or cilium, the basal linking structures *in toto*, presumably including the inter-triplet linkages of the basal body when it is present, are important mechanically for motility; on the basis of the experiments reported here, it is proposed that their effect – however it is achieved – is both to sustain and to regularize the beating of the axoneme.

Materials and methods

Semen from a group of domestic fowls (*Gallus domesticus*) was collected and pooled. The motility of intact spermatozoa was observed at room temperature (range 16–22 °C) after a 1:1650 dilution of the semen in Hanks' basic salt solution (BSS) containing 1 % polyethylene glycol.

Reactivated motility, in intact spermatozoa, was examined after diluting the semen initially 1:1 in Hanks' solution (for 10 min), then 1:825 in a demembranation solution consisting of 230 mmol l^{-1} sucrose, 15 mmol l^{-1} potassium glutamate, 3 mmol l^{-1} $MgSO_4$, 0.5 mmol l^{-1} EDTA, 1 mmol l^{-1} dithiothreitol, 40 μg ml^{-1} Trypsin inhibitor (from soybean), 1 % polyethylene glycol, 0.04 % Triton X-100 and 20 mmol l^{-1} Tris–HCl buffer (pH 7.9). ATP, typically 500 μmol l^{-1}, was subsequently added.

To amputate the sperm flagella, semen samples were diluted with an equal volume (0.1 ml) of Hanks' BSS in a 10 ml tube, and 10 μl of a solution of Trypsin inhibitor (from soybean, 2 mg ml^{-1}) was added. Each sample was then vortex-sheared for 30 s at 2810 revs min^{-1} (Whirlimixer, Fison Scientific). To compare the reactivated motility of proximal and distal flagellar segments, 5 μl of the vortexed sample was immediately diluted into 1 ml of reactivation solution and examined following the further addition of ATP at an appropriate concentration. Most studies used purified distal segments made by diluting 20 μl of the vortexed sample rapidly into 1 ml of demembranation solution, centrifuging it at 3180 ***g*** for 6 min in an Eppendorf tube and then carefully removing 0.1 ml from the middle of the supernatant. This was the fraction rich in distal flagellar segments.

The use of caged ATP (McCray *et al.* 1980) has not previously been reported for flagellar reactivation. For this, two further additions were made to the demembranation solution: ATP, P_3-1-(2-nitrophenyl)-ethyl ester (caged ATP; Calbiochem) to a final concentration of 1 mmol l^{-1}; and apyrase (Sigma) 0.5 munits μl^{-1}. Apyrase is an ATPase from *Solanum tuberosum* included to remove contaminating ATP from caged ATP. The dithiothreitol in the demembranation solution is necessary as an inhibitor of the 'cage', post-photolysis. The suspension was then placed under a supported coverslip and examined using an oiled dark-field condenser and an oil-immersion ×40 planapochromat, N.A.1 (Leitz). A long-pass filter with a cut-off at 420 nm (Oriel Scientific, no. 59482) was in the filter tray from the start. It was removed by hand whenever ATP release was required. The intensity of light, from a standard 100 W quartz–iodide lamp, was sufficient for photolysis when a dark-field condenser was used. The small size of the illuminated field (diameter 580 μm) and the slow rate of diffusion of ATP meant that many experiments could be performed on a single preparation.

For the study involving micromanipulation, it was impractical to arrange dark-field illumination. Phase contrast was chosen. Therefore, the caged ATP technique could not be used and 0.5 mmol l^{-1} ATP was included in the solution. At least 15 min had to elapse to allow sedimentation, by which time most distal segments were immotile and straight. In the first experiments, unpurified flagellar segments were used; recent work has been with purified distal principal pieces. A 40 μl sample was placed in an open chamber, the floor of which was a silicone-coated coverslip that had been repeatedly washed. Using an inverted microscope and a ×40 phase objective (Leitz, Heine system), attempts were made to compress distal segments of axoneme with a glass microneedle held in a micromanipulator (type TVC500, Research Instruments Ltd, Penryn, England). All the experiments were recorded with a 50 Hz CCD video camera on a VHS video tape. Selected sequences of images have been photographed or traced from the monitor.

Characterizing the purified distal flagellar segments involved immunocytochemistry. The monoclonal antibody (CFS), against fibrous sheath, was raised fortuitously from an antigen preparation of SDS-denatured cockerel sperm flagella. The immunization and fusion were performed using an *in vitro* kit (Immune Systems Ltd, Bristol, UK), as described by Holley (1992). Hybridoma supernatants were screened on demembranated cockerel sperm that had been air-dried and fixed with acetone. (Results of immunoblotting with CFS will be published elsewhere.) Negative staining with methylamine tungstate was carried out following immunogold labelling of the demembranated, acetone-fixed flagella. Purified distal flagellar segments were examined for the presence of fibrous sheath material. FITC-conjugated, anti-mouse IgM secondary antibody (Sigma) was applied for this purpose. A Leitz Orthoplan epifluorescence microscope was used, equipped also with a substage dark-field condenser.

After vortex-shearing, samples of sperm were fixed, pelleted, embedded and sectioned for electron microscopy (see methods in Woolley and Brammall, 1987). Transverse profiles of axonemes were examined for the presence or absence of plasma membrane.

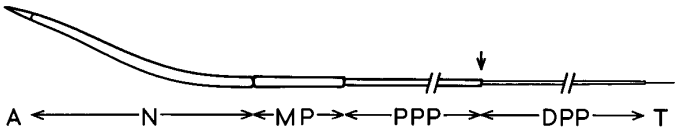

Fig. 1. Diagram of the spermatozoon of *Gallus domesticus*. A, acrosome; N, nucleus; MP, midpiece; PPP, proximal principal piece (axoneme enclosed in fibrous sheath); DPP, distal principal piece (9+2 axoneme only); T, tip of flagellum. The dimensions are given in the text. When a preparation of distal segments is made by vortex-shear, and then purified, they are almost all found to have broken off distal to the end of the fibrous sheath (arrowed).

Results

Establishing the length and structure of the flagellar segments

The structure of the sperm flagellum of *Gallus domesticus* has been reported (reviewed by Thurston and Hess, 1987) but will be restated briefly (see Fig. 1). Its basal body (distal centriole) is 1.7 μm long, occupying the proximal half of the mitochondrial section or midpiece; it consists of triplet microtubules embedded in dense material that is continuous proximally with the connecting piece and distally with accessory (dense) fibres that run alongside the axonemal doublets for approximately 2 μm. The proximal principal piece (PPP) of the flagellum is defined by the presence of a tapering, cylindrical fibrous sheath. Then, after the sheath terminates, there is a long region of simple '9+2' axoneme referred to here as the distal principal piece (DPP). In the short tip region, the axoneme is progressively simplified (Woolley and Brammall, 1987).

In this work, we set out to study the motor capabilities of lengths of '9+2' axoneme separated from their basal bodies and other accessory structures, i.e. the section DPP-T in Fig. 1. However, the boundary between the DPP and PPP (Fig. 1, arrow) cannot be recognized dependably by light microscopy.

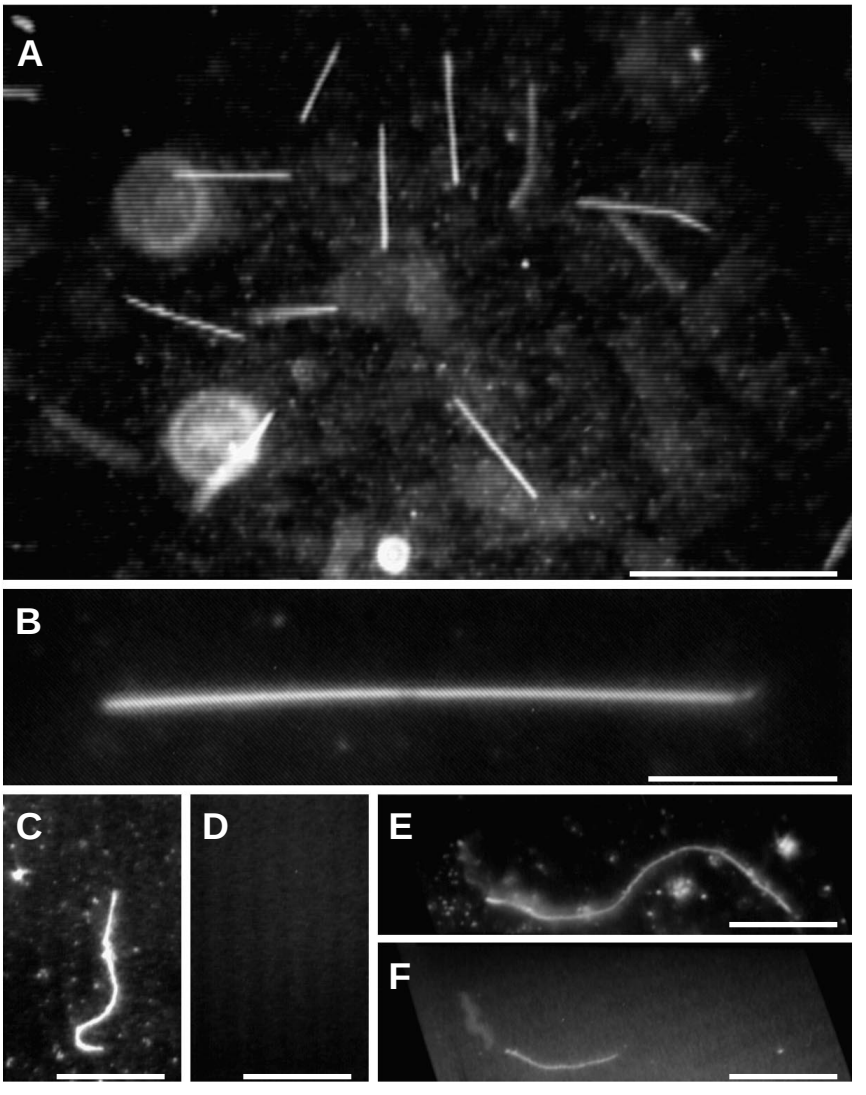

Fig. 2. Video-images, dark-field illumination. (A) Preparation of purified distal flagellar segments, in suspension, incubated in 500 μmol l^{-1} ATP for 20 min. Most of the segments were immotile and straight by this time. Scale bar, 50 μm. (B) Individual distal segment, as in A, but photographed using a $\times$100 objective to demonstrate the tip of the flagellum, at the right. The apparent thickening towards the left-hand end is because the specimen deviates from the plane of focus. Scale bar, 10 μm. (C) Distal segment incubated with anti-fibrous-sheath monoclonal antibody and then FITC-conjugated secondary antibody, illuminated by substage dark-field condenser. Scale bar, 25 μm. (D) A control micrograph of the same field with epi-illumination from an ultraviolet source. No fibrous sheath material is revealed. Scale bar, 25 μm. (E) Entire spermatozoon incubated with anti-fibrous sheath antibody and then stained as in C, illuminated by substage condenser. Scale bar, 25 μm. (F) The same field, showing the fluorescence of the fibrous sheath by ultraviolet epi-illumination. (The nucleus, which is partially dispersed by the preparation method, is weakly fluorescent.) This use of the anti-fibrous sheath antibody allowed the lengths of the proximal and distal segments of the principal piece to be determined (see text). Scale bar, 25 μm.

Therefore, we have used several methods, two of them indirect, to confirm the identity of putative DPP-T isolates (Fig. 2A,B). First, by immuno-staining the fragments with an anti-fibrous sheath monoclonal antibody, we have shown that of 83 purified DPP-Ts examined only three (3.6 %) actually included short regions of PPP (Fig. 2C,D). Second, we used the same antibody to obtain an estimate (by difference) of the length of the DPP-T segment in intact sperm (Fig. 2E,F); the length distribution in a sample of 330 putative DPP-T segments was then related to this known actual length (Fig. 3). From a pooled sample of 25 spermatozoa, the measured lengths (means ± sample S.D.) were: entire flagellum 81.48±1.28 μm, PPP 25.78±0.98 μm, midpiece 3.82±0.49 μm and DPP-T (by subtraction) 51.88 μm. It is clear from the negatively skewed distribution in Fig. 3 that very few (3 %) of flagellar segments in the purified DPP-T fraction exceeded the known mean length of that region. Both these approaches depended on the specificity of our monoclonal antibody for fibrous sheath protein, which has been demonstrated by electron microscopy (Fig. 4). The third observation supporting the claimed identity of DPP-T segments was that a tapering tip, about 1 μm long, could be seen in most (e.g. 17 out of a sample of 22) by dark-field illumination (Fig. 2B).

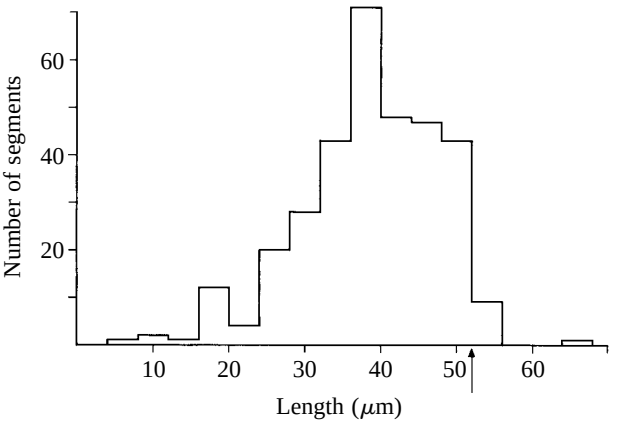

Fig. 3. Frequency distribution of flagellar segment length for purified preparations of amputated segments. The sample (*N*=330) was pooled from two experiments, each of which used semen pooled from several birds. The modal length is close to half the length of the flagellum. Few amputated segments exceed the calculated mean length of the distal principal piece (arrowed). Note that the distribution is negatively skewed in relation to this value.

Reactivation of intact spermatozoa

The normal motility of *Gallus domesticus* sperm flagella is always three-dimensional and so it cannot be described in terms of the planar bending of echinoderm and other spermatozoa. However, roll frequency can be determined and beat frequency can sometimes be detected from the regular rocking motion of the midpiece region. An impression of live sperm motility can be obtained from the example in Fig. 5A–C. This sequence illustrates the propagation of a bend on the distal flagellum: such bends are typically of short arc length, with long interbend regions, giving bend sequences an angular rather than an undulatory appearance. (When bovine serum albumin is present, the waveforms are more helicoid; see Woolley and Brammall, 1987.) After demembranation and reactivation from rigor, using caged ATP, 98 % of a sample of such sperm (*N*=52) began to swim. An example of reactivated motility chosen to show bend propagation on the distal flagellum is presented (Fig. 5D–F). From images such as those in Fig. 5, bends on the distal flagellum appeared to have a typical angle of approximately 25 ° (0.44 rad).

Reactivation of proximal and distal flagellar segments

The vortex-shear treatment essentially breaks the sperm into proximal and distal segments. In general, the proximal segment, which usually retains the head, continues to swim vigorously, which must mean that the cell membrane reseals after the breakage of the flagellum. The distal segments are immotile by the time they can be examined, having presumably exhausted the available ATP. Electron microscopy of thin sections of pellets of vortexed sperm confirmed the persistence of the cell membranes (the images are not shown). After demembranation, it was possible to reactivate more than 80 % of the proximal flagellar segments – defined by the presence of the sperm head. Their motility was vigorous and persistent (Figs 6 and 9).

The potential for reactivation of the distal flagellar segments, which is the main subject of this paper, has been studied using purified preparations of DPP-Ts, as characterized in the

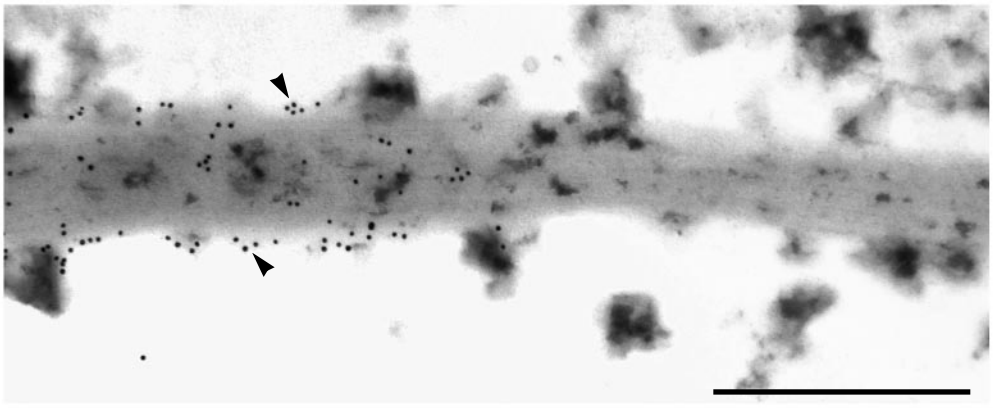

Fig. 4. The junction between the proximal (left) and distal parts of the principal piece, seen in a whole mount, by electron microscopy. The sample had been demembranated, acetone-fixed and immunogold-labelled using the CFS antibody, prior to staining with methylamine tungstate. The gold labelling (arrowheads) is confined to the fibrous sheath of the proximal principal piece (at left). Scale bar, 0.5 μm.

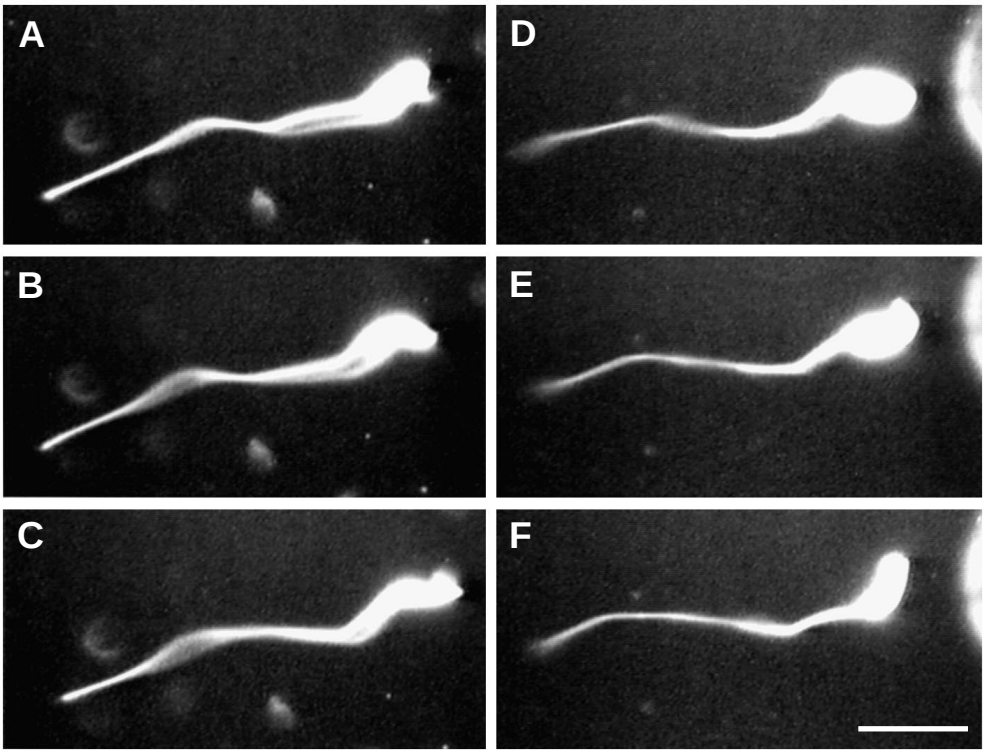

Fig. 5. Video-images, dark-field illumination. Progressive motility in intact (living) and demembranated (reactivated) spermatozoa. (A–C) Intact, living spermatozoon, consecutive frames (interval 20 ms). Sequence chosen to show a bend propagating on the distal flagellum. Under the conditions of recording, this particular cell had a progressive velocity of 8.7 μm s^{-1}, a roll frequency of 8.9 Hz and a beat frequency of approximately 8.5 Hz, these values being typical. (D–F) Demembranated (reactivated) spermatozoon, shown similarly, also to demonstrate a bend propagating on the distal flagellum. Progressive velocity 8.6 μm s^{-1}, roll frequency 10.2 Hz, beat frequency approximately 10.3 Hz. Scale bar, 25 μm.

preceding section. When the reactivation of these was witnessed individually, using the caged ATP/apyrase method, the first few seconds of exposure to ATP caused almost all the DPP-T segments to become motile. Their motion can be described briefly as 'irregular beating', a self-contradictory phrase that requires explanation. Initially, when in rigor, most of the distal segments displayed bends. As the ATP concentration rose, the segments usually straightened significantly before new bend formation occurred. New bends, of small angle, then arose – typically in mid-segment. The position of the crests of such bends then moved towards the tip (Fig. 7). Although it could not be demonstrated formally, the bends appeared to maintain their angle as they travelled. Bends of apparently opposite direction behaved in the same way (Fig. 7). The problem of specifying this 'irregular beating' may be judged from Fig. 8, which shows that flagellar shapes recur, with alternations of bend direction; there are clearly short periods of regularity but also intermittency, the whole picture being complicated by three-dimensionality. Fig. 8 demonstrates what is meant here by 'irregular beating'. In the time taken to prepare a slide of distal segments in 500 μmol l^{-1} ATP, however, the proportion motile had declined to about half, and continued to decline exponentially (Fig. 9). The decline was not due to the exhaustion of the ATP, since proximal flagellar segments continued to swim throughout similar, parallel incubations (Fig. 9). Also, the poor motility of the distal segments and its rapid decline were not due to a difference in the optimum ATP concentration for the proximal and distal segments of the flagellum (Fig. 10). Thus, to summarize, after a brief exposure to ATP, a large majority of the distal flagellar segments became immotile and straight (quiescent) (see also Fig. 2). In this context, motility was defined as any perceptible repetitive bending noticed during a 1–2 s pause in scanning the field. It is emphasized that qualitatively, the motility of the proximal and distal parts of the flagellum was very different – that of the distal segments (DDP-Ts) was definitely abnormal, being much less regular and less well coordinated, as described above.

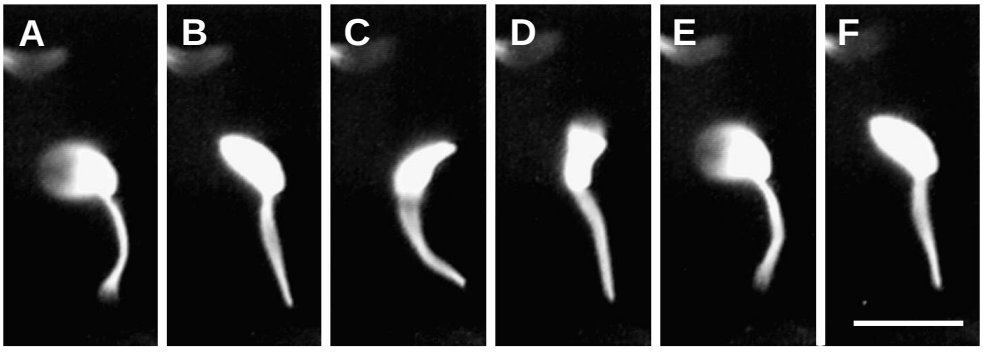

Fig. 6 (A–F) Video-images, dark-field illumination, showing a sequence of images selected to show the regular rolling and beating of a proximal sperm segment, demembranated and reactivated, after amputation of the distal part. Progressive velocity 3.6 μm s^{-1}, roll frequency 2.0 Hz, beat frequency 9.7 Hz. The interval between A and E is 0.5 s. Scale bar, 25 μm.

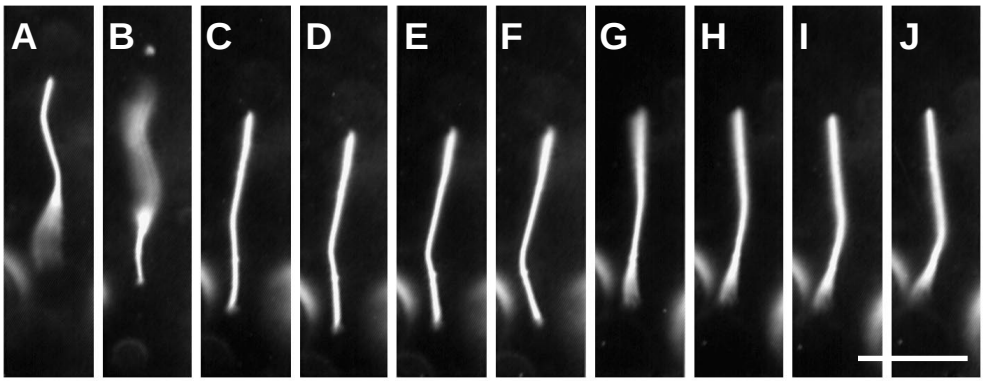

Fig. 7 (A–J). Video-images, dark-field illumination, showing the distal segment: initial response to ATP release from caged ATP. (A,B) Rigor state, a three-dimensional shape focused at two levels; (C–J) following release of ATP from caged ATP, bend propagation on each side of the segment, at 20 ms intervals (F–G interval was 3 s in order to capture the clearest images). Scale bar, 25 μm.

A second reactivation of distal segments, after they had become quiescent

When quiescent, straight distal segments (i.e. having been incubated in 500 μmol l^{-1} ATP for 15–20 min) were put into samples of caged ATP/apyrase, they returned to the rigor state as the ATP was depleted. (Parallel experiments, using the motility of proximal fragments as a bioassay for ATP, showed that its concentration dropped from 500 μmol l^{-1} to less than 20 μmol l^{-1} in approximately 1 min.) This procedure re-established various bends on the formerly straight distal segments, perhaps owing to inhomogeneities in apyrase concentration during the mixing of solutions, together with the physical effects of the mixing. When such distal segments were then re-exposed to ATP by photolysing caged ATP, they again displayed transient, feeble motility (Fig. 11; Table 1). Thus, the phenomenon depicted by the filled symbols in Fig. 9 could be re-enacted after curvatures had been re-imposed on the distal segments.

Re-initiation of motility in quiescent distal segments by micromanipulation

The intention of this experiment was to compress the axoneme segment at one end against the base of the chamber and thus to simulate a resistance to intra-axonemal displacements crudely comparable to that normally effected by the basal structures. In these experiments, the flagellar tips could not be seen by the (imperfect) phase-contrast illumination, so the polarity of the segment could not be decided. In fact, direct visualization was scarcely possible and the whole experiment was monitored on the video screen. Some of the early attempts were on unpurified flagellar fragments, but all the results have recently been

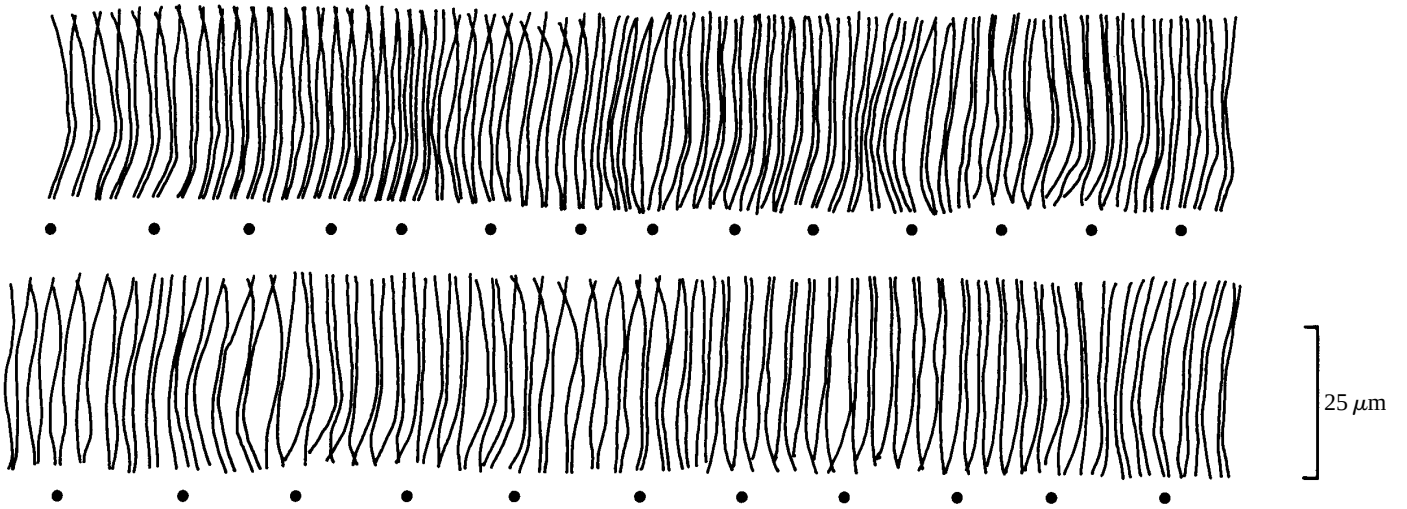

Fig. 8. Tracings from a sequence of video-frames demonstrating the initial phase of the reactivation of motility in a distal flagellar segment. For comparison, the specimen is the same as that in Fig. 7. The ultraviolet barrier filter had been removed 4 s prior to the start of these tracings, so that the movement was already established. Tracings were made of every fifth frame i.e. at 0.1 s intervals. To assist interpretation, the black spots indicate equal time intervals of 0.5 s. The edges of each flagellar image have been drawn, with the thickness of the image increasing as the specimen moves out of the plane of focus. This sequence illustrates the type of motion and the difficulty of describing it quantitatively on account of its three-dimensionality. There is a reasonably clear recurring pattern in the upper part of the figure: it appears to be a rhythmic beating with a period of approximately 1.5 s. But this becomes difficult to follow as the bends start to occur orthogonally to the plane of focus (middle of lower row). The displacement of bend crests towards the tip (lower end) is characteristic and is seen in several places (e.g. in the first few tracings of each row of the drawing).

Table 1. *Amputated distal flagellar segments: the recovery of beating*

Experiment	A Proportion of distal segments that beat on initial exposure to ATP (from caged ATP)	B Proportion of sample A still motile after 20 min of exposure to 500 μmol l^{-1} ATP in the medium	C Proportion of sample B that beat after sudden depletion of ATP and re-release of ATP (from caged ATP)
1	0.77 (*N*=35)	0.09 (*N*=79)	0.63 (*N*=27)
2	0.58 (*N*=57)	0.07 (*N*=76)	0.74 (*N*=47)
3	0.69 (*N*=48)	0.06 (*N*=124)	0.53 (*N*=43)

The effect in C depends upon curvatures being re-established on the straight immotile segments of B.

The figures in columns A and B can be considered to be further confirmatory data points for Fig. 8, filled symbols, at times zero and 20 min, respectively.

repeated on purified distal segments (DPP-Ts) as characterized above.

We selected distal segments that were lying upon or close to the coverslip that formed the base of the chamber. As expected, by the time they had sedimented, these were straight and immotile in the presence of 500 μmol l^{-1} ATP. Compression at one end was attempted upon 258 distal segments, of which 169 (65 %) were judged to have made a definite, active response. Of these, 12 responses involved the formation of one bend or one cycle of bending and are not considered further. The remainder (157) responded immediately to the touch of the needle with cycles of bending that were sufficiently rhythmical that a beat frequency could

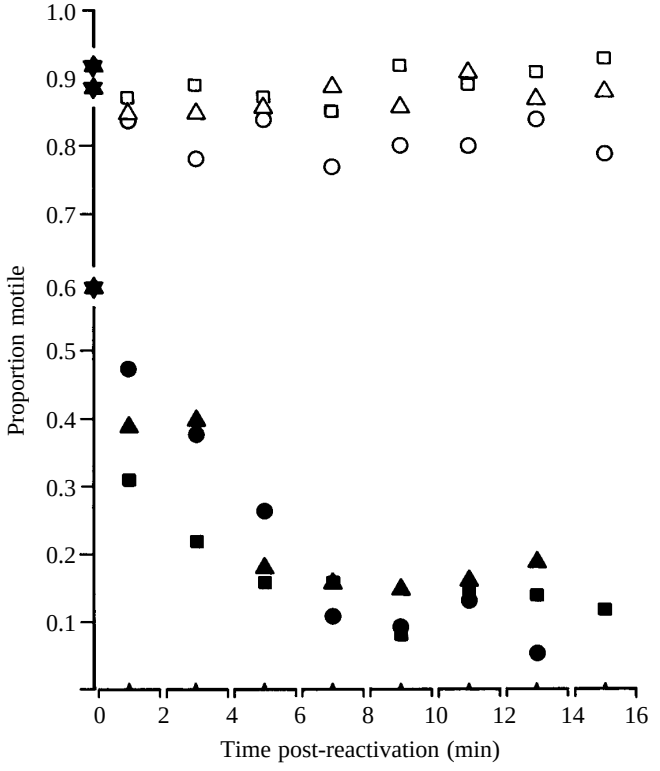

Fig. 9. The persistence of reactivated flagellar beating in proximal segments (open symbols) *versus* purified distal segments (filled symbols). There are three experiments in each series. All data points represent the result of bulk addition of ATP at 500 μmol l^{-1} except for the three filled symbols on the *y*-axis (time=0), which show the motility of distal segments during the first 5 s following photolysis of caged ATP; these three points are based on 22, 26 and 52 specimens. All other points are based on 100–150 specimens. The definition of 'motile' included all perceptible oscillatory motion, however feeble.

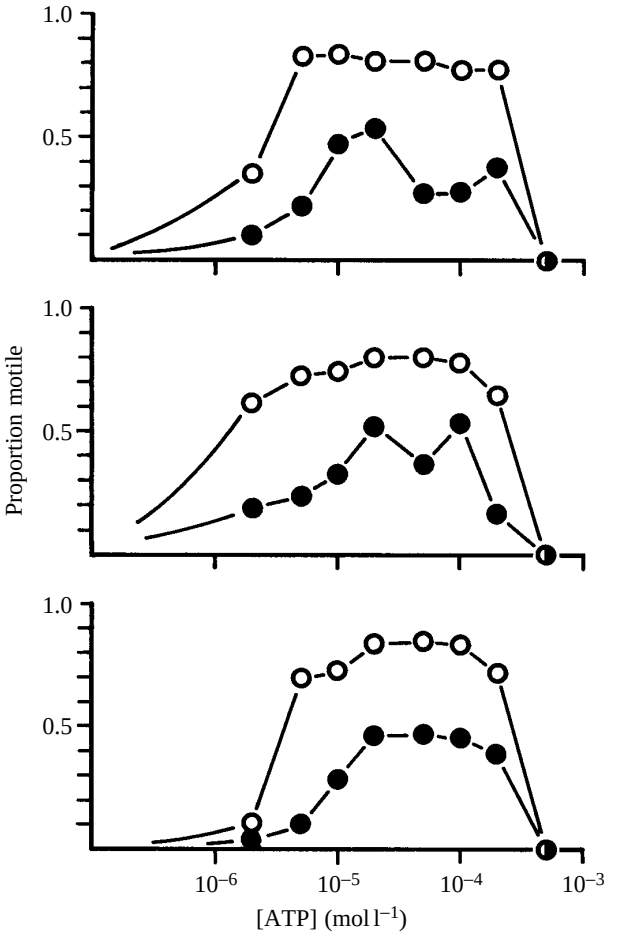

Fig. 10. The effect of ATP concentration on the motility of proximal segments (open symbols) *versus* distal segments (filled symbols). Three experiments were performed. Each data point represents 40–140 specimens, examined for 1–2 s each during the first 5 min of reactivation. Motility in the absence of ATP was always zero.

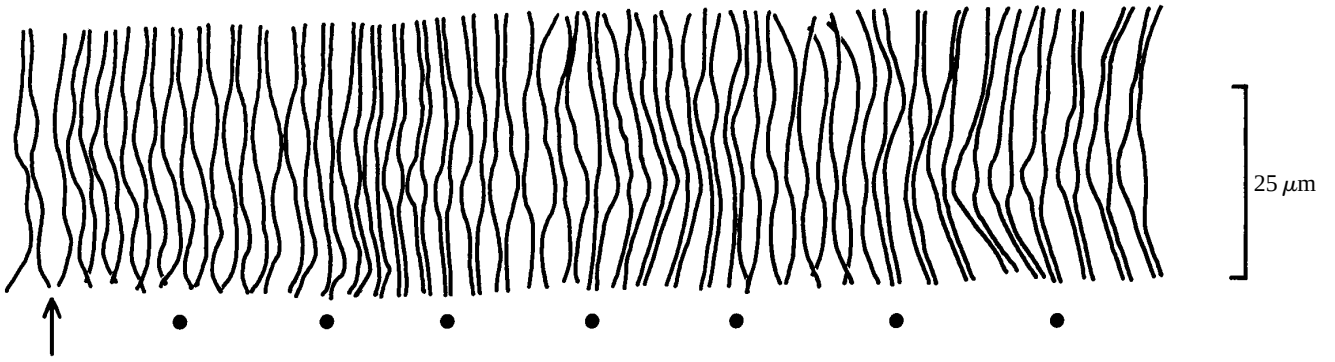

Fig. 11. Tracings from a sequence of video frames demonstrating the initial phase of the reactivation of a distal segment for a second time (see text). The ultraviolet barrier filter was removed at the arrow, after which tracings were not made for the next 0.5 s. Thereafter, the images are at 0.1 s intervals, as for Fig. 8.

usually be assigned (on frame-by-frame replay) on the basis of the repetitive reappearance of the waveforms. These responses have been divided into two groups (i) those where the entire flagellum beyond the compression point was free to move, designated 'free' segments, and (ii) those, where the flagella, when they became active, were clearly seen to be already attached to the substratum at another position, usually the other end, designated 'attached' segments.

In the present context, the responses of the 'free' segments are more significant. Recordings of 73 such responses were obtained, of which 63 were of sufficient amplitude and clarity on replay to be analysed. Each response was followed for as many cycles as possible to a maximum of 20; the mean number of cycles actually observed was 10.62 per segment. The mean cycle frequency was 4.51±1.72 Hz (sample S.D.; N=63). Thus, the average segment in this series was timed for 2.35 s, but this is not a measure of the intrinsic persistence of the response, since many responses were ended by lifting the microneedle. We have not attempted to analyse the detailed geometry of the cycles of bending on account of the problem of three-dimensionality. In general, the bends were of low amplitude (Fig. 12); in-focus bends showing small bend angles are captured in Figs 13 and 14. In 15 definite instances, the axoneme continued to beat after the microneedle was lifted (Figs 12, 13). We took this to indicate that the axonemal structures had been permanently interlocked through being stuck down onto the coverslip. In other examples, after a period of induced beating the flagellar segment slipped away from the needle (Fig. 14), leading to an almost immediate straightening, without further bend initiation. In 29 out of 63 instances, it was possible to be sure of the direction in which induced bends travelled: this was away from the site of compression in 25 cases (Fig. 14) and towards the needle in the other four (Fig. 15).

The 'attached' distal segments, not illustrated here, displayed bending between two fixed points. There were 84 examples, of which 63 were analysed. Their mean frequency was 5.96±2.91 Hz (S.D.; N=63), a value significantly greater than for the 'free' segments (P<0.001, assuming normality).

Discussion

The initial and second reactivations of distal segments (without micromanipulation)

Owing to the use of caged ATP/apyrase, it is possible to say that almost all distal segments display motility when ATP is first liberated. It is safe to assume that this motility occurs in the absence of the structures that occur in the basal and proximal flagellum. Should our initial hypothesis (that a basal resistance is a requirement for motility) be retained?

It would be possible to defend the hypothesis by arguing that, when the flagellum is broken, structures become enmeshed at the fracture site so as to act together as a new basal-end resistance (a 'damage-resistance'). It should be noted that damage, as caused by microneedles in the later part of our study, can have this effect.

However, our experiment to induce a 'second reactivation of distal fragments after they had become quiescent' is viewed as a test of this possibility. In consequence of it, we prefer not to accept this explanation but to reject the original hypothesis. The argument, which is not fully conclusive, is as follows: (i) if a 'damage-resistance' is supporting the motility, then when motility ceases (quiescence) the 'damage-resistance' is no longer acting (i.e. the enmeshed structures may have been loosened by activity); (ii) quiescent flagellar segments are put back into rigor without further breakage and probably without further damage; (iii) nevertheless, these formerly quiescent segments will beat again for a few cycles, if they have acquired bends passively while being returned to rigor.

On the strength of this reasoning, we consider that axonemal motility, of a weak and irregular kind, can occur independently of a localized resistance and that it is facilitated in some way by energy already stored in pre-existing bends. Motility of this type, however, is very short-lived, suggesting that, without the basal structures, the energy stored elastically in the flagellum cannot be replenished and the flagellum settles into quiescence and straightness.

Re-initiation of motility in quiescent distal segments by micromanipulation

This refers to the compression of one end of a quiescent

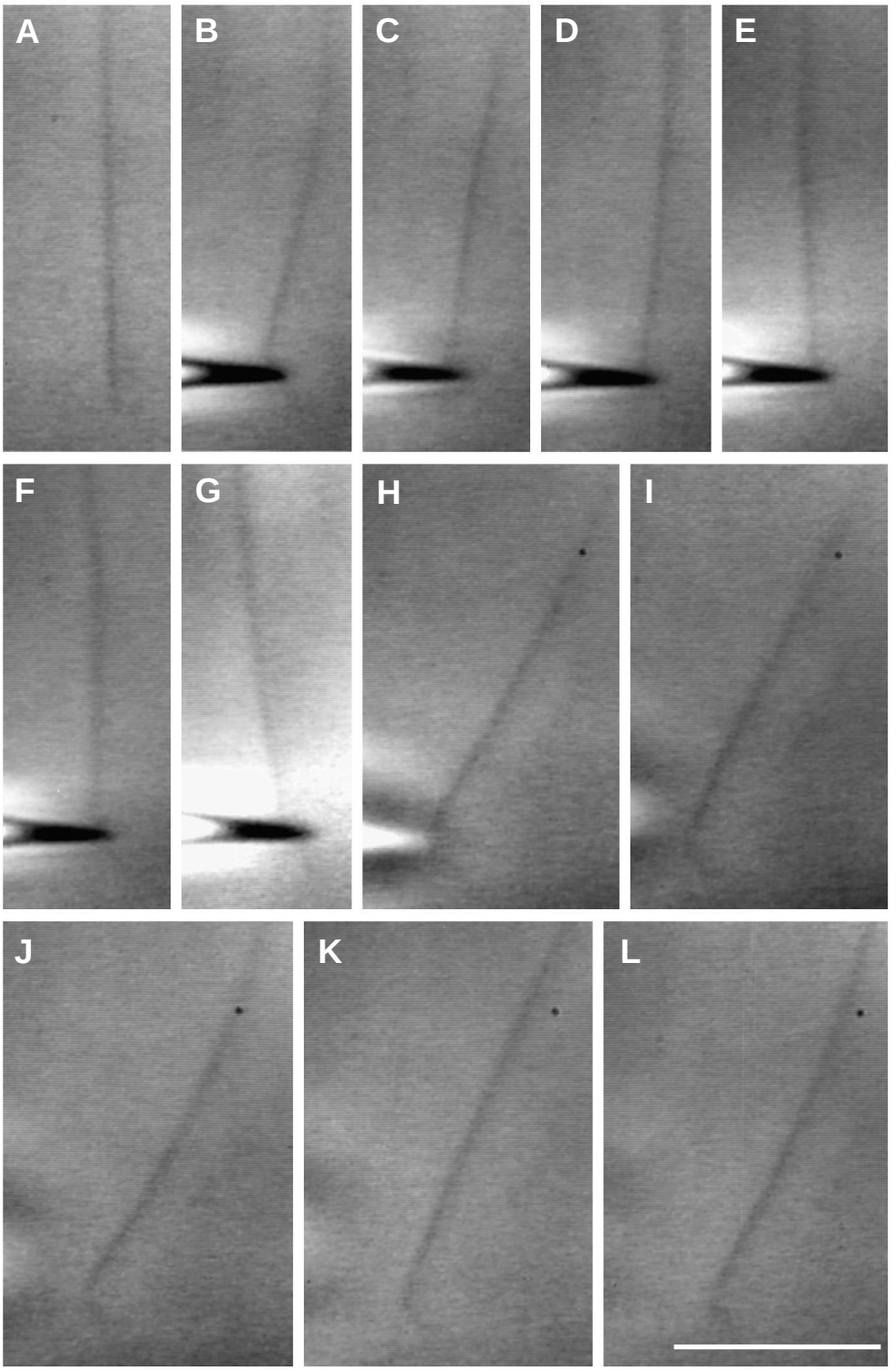

Fig. 12. Video-images, phase-contrast illumination. This sequence shows (A) one end of a quiescent distal flagellar segment in reactivation solution; (B–G) representative images of the oscillatory response to compression; the frequency, timed over 19 cycles, was 8.5 Hz; (H–L) the continuation of beating, needle lifted, axoneme remaining stuck down on the coverslip. For clarity, the frames have been selected to emphasise two-dimensional phases of the beat cycle. The sequence B–G occupied 4.7 s. A further 5.2 s elapsed between G and H, during which the flagellum swung to the right. The sequence H–L occupied 0.28 s. Scale bar, 10 μm.

distal segment in the continuous presence of ATP and to the movements made in response when the rest of the flagellum is unattached to the base of the chamber.

The functional status of 'quiescent' flagellar segments is not understood, though it is of considerable interest. The fact that rapid beating can be induced in quiescent segments by compression indicates that the motor system within the segment is essentially intact, but it is not clear whether the dynein motors are in an active state before compression or whether they are triggered into activity by compression. In the first case, the resistance due to compression perhaps transforms sliding that is already occurring into the first bend, meaning either that no other resistances in the flagellum are adequate for this or that the bending moments are all diametrically opposed and in exact balance. In the second case, one imagines the distal segments held straight passively, through the

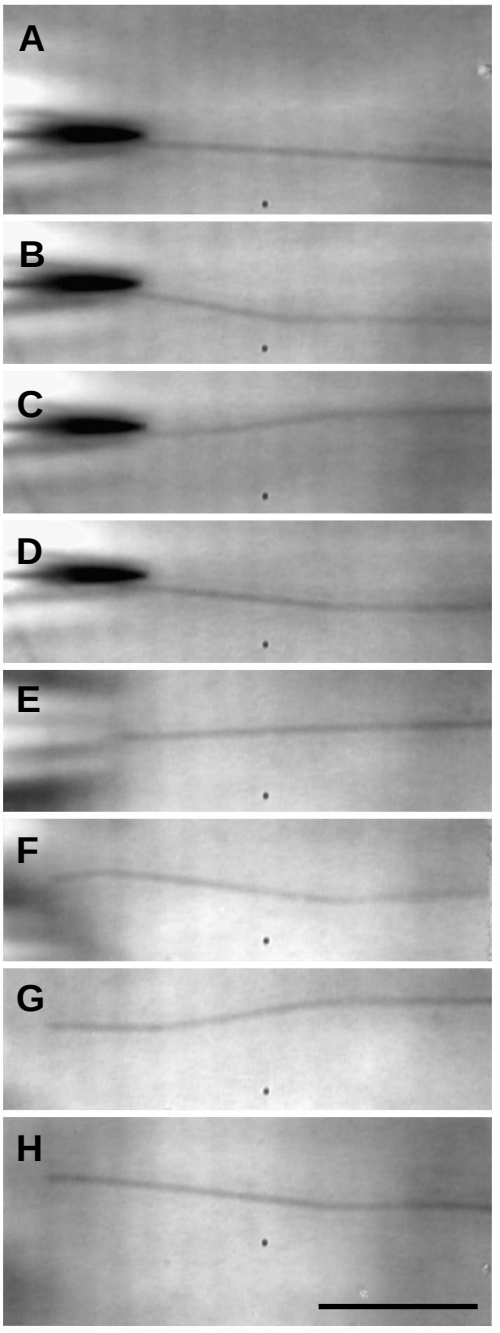

Fig. 13. A second example of compression-induced beating, persisting after raising the microneedle. In this case, the bends are mainly two-dimensional and were seen from the full video sequence to be travelling away from the needle (not demonstrated in this figure.) The images A–H were selected for their clarity in showing the oscillation; the frequency, timed over 12 cycles, was 5.0 Hz. Scale bar, 10 μm.

diametrically opposed vectors of torsional tension exerted by the nine doublet microtubules themselves. This suggestion is based on the uniformly sinistral helicality of individual doublets isolated from these and other axonemes – discussed by Woolley and Brammall (1987). Under these conditions, compression would activate effective sliding. The implication here is that the motor system is load-sensitive. When the basal region is removed, all the doublets can perhaps be moved slightly backwards and forwards as a result of 'weak' cycling of the arms. This would correspond to the small-scale ATP-dependent linear oscillation of individual doublets detected by Kamimura and Kamiya (1989, 1992). It may well represent ATPase activity uncoupled from bending, as reported for broken flagella by Brokaw and Simonick (1976). In the presence of the basal region, or when quiescent distal segments are compressed with a needle, the dynein arms (or a subset of them) may detect a firm resistance to the sliding of the doublet adjacent to them, perhaps through a deformation of the tenuous B-linkage (Burgess *et al.* 1991) and, only then, in response to the lowered compliance, engage in full force generation. This scheme is of course speculative. In the following subsection, it is suggested that the effect of compression is general rather than local.

An important practical question is whether extraneous low-amplitude mechanical vibrations might have been transmitted through our microneedles so as to entrain the beating of the flagellar segments. Since we have no recordings of such vibrations, we cannot deny that vibrations of sub-visible amplitude may have been transmitted at the moment of contact. However, flagellar segments often remained attached to the slide and continued beating after the needle was lifted. This shows that the beating is at least self-sustaining.

Many quiescent, straight distal segments, when they began beating in response to compression were seen to be attached to the base of the chamber at their other end. There are at least three explanations for how this was possible: (i) the motion of the needle included a slight push such as to create a curvature of the axoneme between the two fixed points; (ii) the induced bending activity dragged the far-end attachment closer; or (iii) the induced sliding activity succeeded in effectively lengthening the segment. We have not tried to distinguish between these possibilities. Rapid oscillations, usually of very low amplitude, ensued. This phenomenon is considered to be quite different from what has already been discussed, since these axonemal segments were prevented from straightening. It is already known that when a bend is induced on a distal axonemal segment it will be propagated (Okuno and Hiramoto, 1976). If such a bend cannot 'run off' the tip, because of adhesions there, the resolution of shear displacement would involve torsion, creating bending in other planes and so perpetuating a complex vibrational motion.

Some features of the bending induced by localized compression

When distal segments were compressed the bending that followed was typically three-dimensional, even though the axoneme was adjacent to a surface. The repetitive occurrence of waveforms did allow the frequency to be estimated: the mean value 4.5 Hz is of the same order as that seen in whole flagella. But it was not feasible to analyse the geometry of the bends. In general, we can report that they were of small angle, often with bent and straight segments similar to those

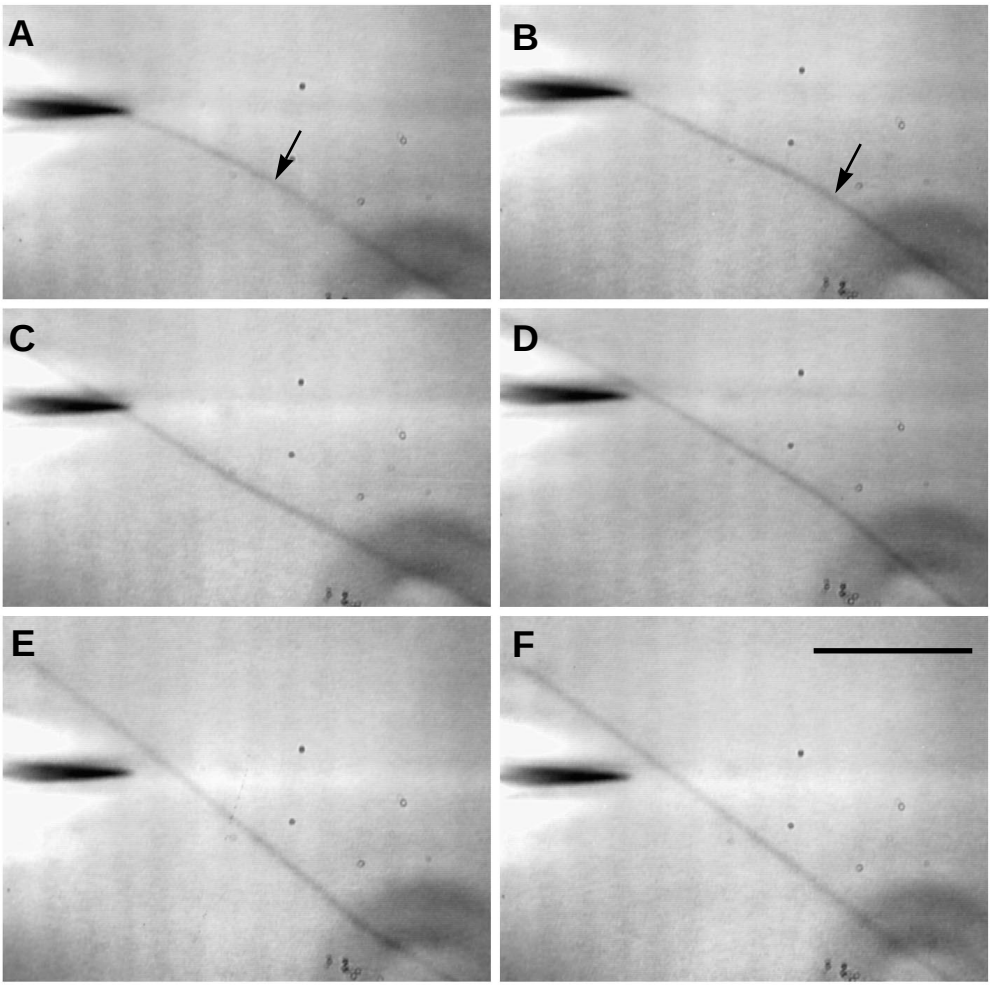

Fig. 14. In this example of compression-induced distal flagellar beating, it can be seen that the crests of the small-angle bends were travelling away from the point of compression. From the bend crest (arrowed) in the consecutive frames A and B, the speed of travel was approximately 170 μm s^{-1}. An opposite bend, 80 ms later, is seen in C; from the actual video sequence, this bend was also moving away from the point of compression. During this period, the frequency, timed over 15 cycles, was 6.1 Hz. Then the axoneme slipped away from the needle at D. From the full video sequence, the bend in D was also seen to travel away from the needle, as did another seen in E; thereafter the axoneme, as in F, remained inactive and straight. Time interval D–F is 100 ms. Scale bar, 10 μm.

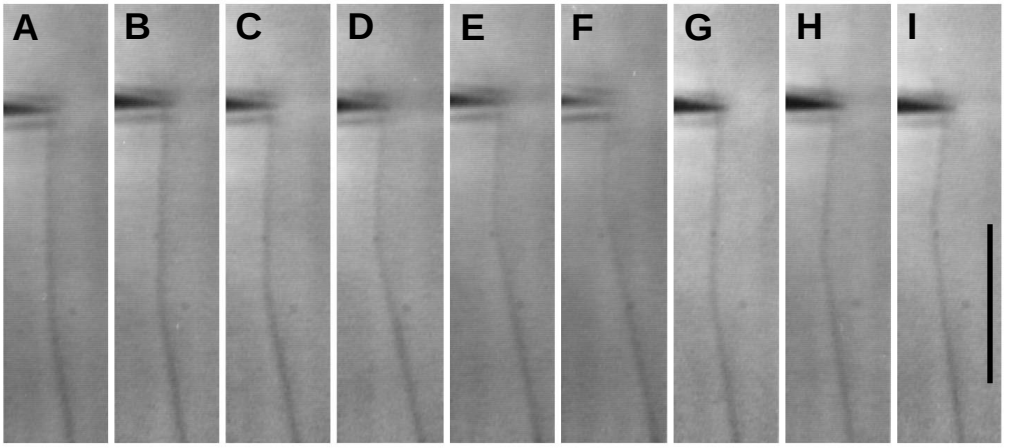

Fig. 15. An example of compression-induced flagellar beating to demonstrate that bend crests in some axonemal segments were found to travel towards the microneedle. In the sequence A–F, a small-angle bend crest moves towards the needle at approximately 28 μm s^{-1}. After an out-of-focus interval, another similar bend crest, in the sequence G–I, also travels in the same direction at approximately 39 μm s^{-1}. The successive images A–I are at the following intervals 20, 40, 80, 20, 40, 1260, 60 and 60 ms. After these two cycles at 1.3 Hz, a further 10 cycles were timed at 5.6 Hz. Scale bar, 10 μm.

seen in locally reactivated sea urchin sperm by Shingyoji *et al.* (1977).

Compression-induced bends moved along the axoneme. In terms of sliding filament theory (Gibbons, 1981), the true propagation of a bend occurs with the bend angle maintained (metachronal sliding); otherwise bend displacements can be expressions of bend growth or relaxation (interbend growth or decay). Thus, since we are unable to analyse the three-dimensional geometry, we do not have proof of propagation and can speak only of the unidirectional movement of bends (bend-crests). Nevertheless, an observation of potential interest was made, namely that in a small number of cases (four), the

bends travelled *towards* the needle. It follows that the effect of the imposed resistance must be transmitted through the axoneme, allowing the intrinsic directionality to be expressed; the site of compression does not itself determine the directionality. This conclusion obviously requires confirmation. The small number of confirmed instances is thought to be due to the difficulty of interpreting the images of low-amplitude bends moving towards a point of obstruction to sliding.

Conclusions regarding the functional importance of the basal region of cilia and flagella

Attention is drawn to the finding that reactivated motility in separated distal flagellar segments is soon lost but can be restored by pressure applied with a microneedle. We assume from this that the crudely applied pressure creates a resistance to sliding between the structures of the axoneme at the point at which it is applied. We suggest that it is this resistance that enables beating to resume and is, further, responsible for the improvement in coordination and vigor over what had been seen, transitorily, in the absence of applied pressure. The inference we make is that, in the intact flagellum and cilium, it is the basal structures, as a group, that provide the localized resistance and, by acting in this way, are necessary for normal axonemal motility. A similar conclusion was reached by Douglas and Holwill (1972) from their observation that the motility of flagella isolated from *Crithidia oncopelti* became much more coherent if they became attached at one end to the slide.

Thus, the *need* for a resistance to sliding at the flagellar base is given further experimental support. The fact that sliding is normally restricted in this region is already well attested, by both functional (Summers and Gibbons, 1971) and ultrastructural (Warner and Satir, 1974) studies. The basal resistance should, however, be regarded as a component resistance within a system of resistances. It would seem to have a general effect upon the axoneme, but it appears not to be an essential determinant of repetitive bendings, as judged by the transitory irregular beating described here. The facilitation of such beating by the pre-existence of a bent configuration suggests that energy available in distributed (i.e. pan-axonemal) resistances supports oscillatory movement. Also, it is believed that distributed resistances are important for bend propagation, as shown by the propagation of bends imposed on amputated axonemes (Goldstein, 1969; Okuno and Hiramoto, 1976). It is not known which structures provide distributed resistance. The radial spokes, nexin links and dynein cross-bridges might all act as resistances to shear, given their locations. Yet the spokes are evidently not essential for bending or propagation in those axonemes that do not contain them (Huang *et al.* 1982; Gibbons *et al.* 1983), and it has recently been questioned whether the nexin links deform elastically when inter-doublet sliding occurs (Bozkurt and Woolley, 1993).

By advocating the functional importance of the basal region, as providing a necessary mechanical resistance, no serious discord with earlier experimental results arises. Since no particular basal structure is specified, different basal linkages could operate in different axonemes. Thus, where cilia are detached from their basal bodies (reviewed by Goldstein, 1974), there is evidence that at least part of the transition zone remains with the cilium. This zone includes a set of 'peripheral links', inter-doublet bridges apparently distinct from nexin (Ringo, 1967). These might be resistive structures. They are clearly distal to the point at which fracture occurs during deciliation of *Chlamydomonas reinhardtii* (Sanders and Salisbury, 1989). In another example, the flagella of *Chlorogonium elongatum*, which are motile when detached from basal bodies, are found to have retained the transition zone structures (Hoops and Witman, 1985). In mammalian sperm flagella, where a transition zone is not typically seen and where the distal centriole degenerates (Fawcett and Phillips, 1969; Woolley and Fawcett, 1973), accessory structures in the sperm neck could provide the resistance, with the sliding force being transmitted *via* dense accessory fibres to the columns of the connecting piece and resisted by the capitulum (as indicated in the work of Lindemann and Gibbons, 1975). Distal centrioles also degenerate in the spermatozoa of some myriapods (e.g. Horstmann, 1968) and of at least seven orders of insects (Phillips, 1970); however, in the extensively studied Lepidoptera and in *Neuronice* sp. (Trichoptera), accessory singlet microtubules appear to be anchored in a nuclear indentation (Phillips, 1970) in an arrangement that could function as a 'centriolar equivalent' (Jamieson, 1987, page 193). In experiments where the entire basal region has been removed by microdissection with needles (Terni, 1933; Lindemann and Rikmenspoel, 1972; Okuno and Hiramoto, 1976), it is possible that any sustained well-coordinated beating in the isolated segment was dependent upon resistance due to compression and compaction caused by the cutting (similar to that seen in our manipulations; see Figs 12, 13). Where the flagellum had been cut off using a pulse from a ruby laser microbeam, as in the influential work of Goldstein *et al.* (1970), the motility was short-lived for another reason (ATP depletion) and it is not clear whether, to explain it, it is necessary to suggest that a new resistance was created by fusion of structures at the abscission site.

Thus, it is proposed that, in simple cilia and flagella, the localized resistance will be created at the base by transition zone links, supported by centriolar inter-triplet links. In some spermatozoa, accessory structures in the neck are probably the main basal, low-compliance resistance. Indeed, any linkages that could prevent inter-doublet sliding, such as the 5–6 bridge of some cilia first described by Afzelius (1959) the 3–8 linkage through the fibrous sheath of the mammalian spermatozoon or the various capping structures at the tips of some axonemes (see Dentler and LeCluyse, 1982) might also, in an auxiliary way, be sustaining effective flagellar beating.

We thank Isobel Coleman and Simon John for assistance during the early phase of this study. Also we are grateful to Debbie Carter and Gini Tilly for the photographic processing. The raising of monoclonal antibodies was supported by a

research grant from the Wellcome Trust; Matthew Holley gave valuable advice and help with this part of the work; Cliff Jeal allowed us to use his utraviolet lamphouse. Geraint Vernon made the important suggestion of using apyrase. Alan Burgess made helpful criticisms of the manuscript. Professor Guttfreund provided an initial gift of caged ATP. We thank Sun Valley Poultry for kindly donating the cockerels. Microdissection equipment had been bought from an AFRC grant to D.M.W.

References

AFZELIUS, B. (1959). Electron microscopy of the sperm tail. *J. biophys. biochem. Cytol.* **5**, 269–278.

BACCETTI, B. (1972). Insect sperm cells. *Adv. Insect Physiol.* **9**, 315–397.

BOZKURT, H. H. AND WOOLLEY, D. M. (1993). Morphology of nexin links in relation to interdoublet sliding in the sperm flagellum. *Cell Motil. Cytoskel.* **24**, 109–118.

BROKAW, C. J. (1972). Computer simulation of flagellar movement. I. Demonstration of stable bend propagation and bend initiation by the sliding filament model. *Biophys. J.* **12**, 564–586.

BROKAW, C. J. AND BENEDICT, B. (1968). Mechanochemical coupling in flagella. I. Movement-dependent dephosphorylation of ATP by glycerolated spermatozoa. *Archs Biochem. Biophys.* **125**, 770–778.

BROKAW, C. J. AND SIMONICK, T. F. (1976). CO_2 regulation of the amplitude of flagellar bending. In *Cell Motility*, Book C (ed. R. Goldman, T. Pollard and J. Rosenbaum), pp. 933–940. Cold Spring Harbor Laboratory.

BURGESS, S. A., DOVER, S. D. AND WOOLLEY, D. M. (1991). Architecture of the outer arm dynein ATPase in an avian sperm flagellum, with further evidence for the B-link. *J. Cell Sci.* **98**, 17–26.

DENTLER, W. L. AND LECLUYSE, E. L. (1982). Microtubule capping structures at the tips of tracheal cilia: evidence for their firm attachment during ciliary bend formation and the restriction of microtubule sliding. *Cell Motility* **2**, 549–572.

DOUGLAS, G. J. AND HOLWILL, M. E. J. (1972). Behaviour of flagella isolated from *Crithidia oncopelti*. *J. Mechanochem. Cell Motil.* **1**, 213–223.

FAWCETT, D. W. AND PHILLIPS, D. M. (1969). The fine structure and development of the neck region of the mammalian spermatozoa. *Anat. Rec.* **165**, 153–184.

GIBBONS, B. H. AND GIBBONS, I. R. (1972). Flagellar movement and adenosine triphosphatase activity in sea urchin sperm extracted with Triton X-100. *J. Cell Biol.* **54**, 75–97.

GIBBONS, B. H., GIBBONS, I. R. AND BACCETTI, B. (1983). Structure and motility of the 9+0 flagellum of eel spermatozoa. *J. submicrosc. Cytol.* **15**, 15–20.

GIBBONS, I. R. (1981). Transient flagellar waveforms during intermittent swimming in sea urchin sperm. II. Analysis of tubule sliding. *J. Muscle Res. Cell Motil.* **2**, 83–130.

GOLDSTEIN, S. F. (1969). Irradiation of sperm tails by laser microbeam. *J. exp. Biol.* **51**, 431–441.

GOLDSTEIN, S. F. (1974). Isolated, reactivated and laser-irradiated cilia and flagella. In *Cilia and Flagella* (ed. M. A. Sleigh), pp. 111–130. London, New York: Academic Press.

GOLDSTEIN, S. F., HOLWILL, M. E. J. AND SILVESTER, N. R. (1970). The effects of laser microbeam irradiation on the flagellum of *Crithidia* (*Strigomonas*) *oncopelti*. *J. exp. Biol.* **53**, 401–409.

HOLLEY, M. C. (1992). A simple *in vitro* method for raising monoclonal antibodies to cochlear proteins. *Tissue & Cell* **24**, 613–624.

HOOPS, H. J. AND WITMAN, G. B. (1985). Basal bodies and associated structures are not required for normal flagellar motion or phototaxis in the green alga *Chlorogonium elongatum*. *J. Cell Biol.* **100**, 297–309.

HORSTMANN, E. (1968). Die spermatozoen von *Geophilus linearis* Koch (Chilopoda). *Z. Zellforsch. mikrosk. Anat.* **89**, 410–429.

HUANG, B., RAMANIS, Z. AND LUCK, D. J. L. (1982). Suppressor mutations in *Chlamydomonas* reveal a regulatory mechanism for flagellar function. *Cell* **28**, 115–124.

JAMIESON, B. G. M. (1987). *The Ultrastructure and Phylogeny of Insect Spermatozoa*. Cambridge: Cambridge University Press.

KAMIMURA, S. AND KAMIYA, R. (1989). High-frequency nanometre-scale vibration in 'quiescent' flagellar axonemes. *Nature* **340**, 476–478.

KAMIMURA, S. AND KAMIYA, R. (1992). High-frequency vibration in flagellar axonemes with amplitudes reflecting the size of tubulin. *J. Cell Biol.* **116**, 1443–1454.

LINDEMANN, C. B. AND GIBBONS, I. R. (1975). Adenosine triphosphate-induced motility and sliding of filaments in mammalian sperm extracted with Triton X-100. *J. Cell Biol.* **65**, 147–162.

LINDEMANN, C. B. AND RIKMENSPOEL, R. (1972). Sperm flagella: autonomous oscillations of the contractile system. *Science* **175**, 337–338.

MACHIN, K. E. (1963). The control and synchronization of flagellar movement. *Proc. R. Soc. B* **158**, 88–104.

MCCRAY, J. A., HERBETTE, L., KIHARA, T. AND TRENTHAM, D. R. (1980). A new approach to time-resolved studies of ATP-requiring biological systems: laser flash photolysis of caged ATP. *Proc. natn. Acad. Sci. U.S.A.* **77**, 7237–7241.

OKUNO, M. AND HIRAMOTO, Y. (1976). Mechanical stimulation of starfish sperm flagella. *J. exp. Biol.* **65**, 401–413.

PHILLIPS, D. M. (1970). Insect sperm: their structure and morphogenesis. *J. Cell Biol.* **44**, 243–277.

RINGO, D. L. (1967). Flagellar motion and fine structure of the flagellar apparatus in *Chlamydomonas*. *J. Cell Biol.* **33**, 543–571.

SANDERS, M. A. AND SALISBURY, J. L. (1989). Centrin-mediated microtubule severing during flagellar excision in *Chlamydomonas reinhardtii*. *J. Cell Biol.* **108**, 1751–1760.

SHINGYOJI, C., MURAKAMI, A. AND TAKAHASHI, K. (1977). Local reactivation of Triton-extracted flagella by iontophonetic application of ATP. *Nature* **265**, 269–270.

SUMMERS, K. E. AND GIBBONS, I. R. (1971). Adenosine triphosphate-induced sliding of tubules in trypsin-treated flagella of sea-urchin sperm. *Proc. natn. Acad. Sci. U.S.A.* **68**, 3092–3096.

TERNI, T. (1933). Microdissection et U.V. microradiopiqure des spermatozoides. *C. R. Ass. Anatomist* **28**, 651–654.

THURSTON, R. J. AND HESS, R. A. (1987). Ultrastructure of spermatozoa from domestic birds: comparative study of turkey, chicken and guinea fowl. *Scanning Microsc.* **1**, 1829–1838.

WARNER, F. D. AND SATIR, P. (1974). The structural basis of ciliary bend formation. Radial spoke positional changes accompanying mocrotubule sliding. *J. Cell Biol.* **63**, 35–63.

WOOLLEY, D. M. AND BRAMMALL, A. (1987). Direction of sliding and relative sliding velocities within trypsinized sperm axonemes of *Gallus domesticus*. *J. Cell Sci.* **88**, 361–371.

WOOLLEY, D. M. AND FAWCETT, D. W. (1973). The degeneration and disappearance of the centrioles during the development of the rat spermatozoon. *Anat. Rec.* **177**, 289–302.